Thin films of photocatalytic TiO_2 and ZnO deposited inside a tubing by spray pyrolysis

M. Miki-Yoshida, V. Collins-Martínez, P. Amézaga-Madrid, A- Aguilar-Elguézabal

Abstract

Thin films of photocatalytic TiO_2 and ZnO were deposited in Vycor tubing by a simple and reproducible spray pyrolysis technique. Films were transparent and non-light scattering. Film characterization by transmission electron microscopy shows that titanium oxide films were polycrystalline and that their structure corresponded to the tetragonal anatase phase. In addition, ZnO films were polycrystalline with a structure that belonged to the hexagonal Wurtzite type. The solar photocatalytic efficiency for butane degradation was compared to that of Degussa P-25 TiO2 powder (P-25). Reaction rate and reaction order were obtained from butane concentration measurements using the tubing as a non-circulating reactor exposed to solar radiation. The best fitting was obtained for a pseudo-first order rate constant. The TiO_2-covered tubing shows very high photocatalytic activity, even higher than that of P-25, if activity per unit of catalyst mass is considered.

Introduction

Since the report of titanium dioxide on the photooxidation of water with a TiO_2 anode [1], many applications based on the photo-electronic properties of this oxide have been developed. Therefore, due to their chemical stability at high temperatures, TiO_2 thin films are used as active material in the electronic conductancetype oxygen gas sensor [2,3]. Furthermore, titanium dioxide films are now widely used in catalysis and photocatalysis [4,5] because of their low cost and other advantageous properties. For

example, they have been used for decomposition of organic contaminants in air and water. Moreover, recent studies have reported bactericidal and detoxification effects of TiO_2 thin films [6,7]. It has been shown that TiO_2-coated materials possess deodorizing, antibacterial, and self-cleaning functions under weak ultraviolet light [8].

Titanium dioxide films can be prepared by many deposition techniques, like sol–gel [9x], atmospheric pressure metal organic chemical vapour deposition [10], reactive cathodic vacuum arc deposition [11], electronbeam evaporation [12], reactive magnetron sputtering [13], static–dynamic films compressed method [14], and spray pyrolysis (SP) [15,16]. Among them, the SP technique has a relatively low cost; it is simple to manipulate, and applicable to large-scale areas. Furthermore, as demonstrated in this study, the technique can be used in thin film deposition on tubing walls.

Photocatalytic TiO_2- or ZnO-covered tubing can be used to decompose organic contaminants andyor to sterilize microbial cells in air or water flows, using solar panel reactors or indoor panels irradiated with UV radiation. This feature renders the photocatalyst-covered tubing applicable to environmental protection, especially in medical facilities and factories manufacturing pharmaceutical and medical devices. In addition, the method described here has a potential application in photothermal solar energy collectors as a way to deposit transparent selective materials.

In this work, we report the preparation of transparent, and non-light scattering thin films of TiO_2 and ZnO inside of Vycor tubing. We have used a simple and reproducible SP technique; to our knowledge, this is the first report about covered tubing obtained by the SP method (see the latest review about SP by Patil in Ref. [17],

and references therein). Only cylindrical photoreactors with thin films deposited by sol–gel technique [18] or with catalyst particles anchored on the walls are reported [5]. Film characterization was done by transmission electron microscopy (TEM) and ultraviolet–visible (UV–VIS) spectroscopy. The photocatalytic efficiency of TiO_2 and ZnO-coated tubing was also compared with that of commercially available photocatalytic Degussa P-25 TiO_2 powder (P-25).

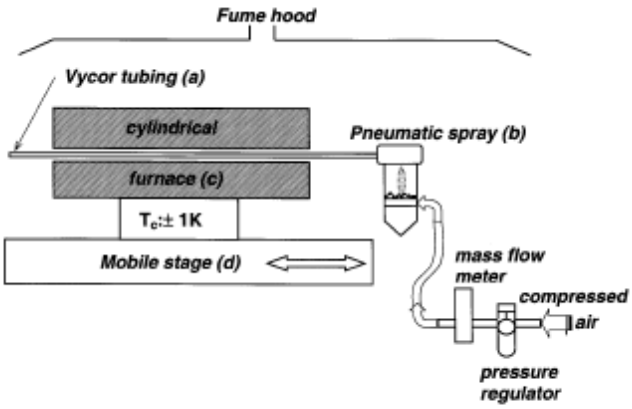

Fig. 1. Schematic diagram of the spraying system. See text for details.

Experimental

Thin film preparation: Titanium dioxide and Zinc oxide thin films were obtained inside Vycor tubing by a new very simple SP technique. The overall dimensions of this tubing were an internal diameter of 7 mm and length of 900 mm. The spraying system is illustrated in Fig. 1. Vycor tubing (a) was attached to a medical nebulizer (b), which was used as an atomizer. This tubing was heated by a cylindrical furnace Thermolyne 1200 (c), with a very precise temperature control (±1 K); the deposition temperature was fixed at 775 K for TiO_2 and at 725 K for ZnO films. The process starts from aerosol generation of precursor solution in the nebulizer. The starting solutions used were a 0.1 mol dm^{-3} dilution of titanyl acetyl acetonate (Merck >98%) (for TiO_2) and zinc acetate (Aldrich

>98%) (for ZnO) in absolute ethanol. This aerosol is subsequently conveyed by the carrier gas, and injected directly into the heated tubing inside the cylindrical furnace. The carrier gas was microfiltered air; pressure and flux were maintained at 310 kPa and 67 cm^3 s^{-1}, respectively. At this stage, optimal conditions of the tubing temperature, chemical parameters, carrier gas nature and velocity are necessary to ensure a deposition reaction and film development. Additionally, the cylindrical furnace was fixed onto a mobile stage (d) which gives it an axial movement, with the purpose of heating sequentially different zones of the tubing; this movement has allowed the production of a uniform film along 70–80% of the tubing length. The rate of furnace displacement was approximately 0.33 mm s^{-1}.

Thin film characterization: UV–VIS transmittance spectra were obtained in a Lambda-10 spectrophotometer. A sample of the filmcovered tubing was cut axially to analyse only one face of the film. Uncovered tubing was also cut to use it as a blank. The beam shape was rectangular (≈6x1 mm^2), its height was aligned with the tubing axis to minimize the effect of tubing curvature. From these spectra, optical transmittances in the UV–VIS region were determined for both external and internal incidence. In addition, the optical interference method was employed to determine thickness and refraction index. TEM analysis was used to evaluate the crystalline structure and morphology of the films. TEM micrographs and selected area electron diffraction (SAED) patterns were obtained in a side entry CM-200 TEM coupled with a DX-Prime X-ray energy dispersive spectrometer. For these studies, the films were peeled off from the Vycor substrate by immersion in diluted HF (5 vol.%); immediately

after, they were floated and rinsed in deionized water; and finally, they were mounted on 1000 mesh copper grids.

Photocatalytic activity measurements: Photocatalytic studies were performed in similar Vycor tubing with an internal volume and geometric internal surface of 32.7 cm^3 and 187 cm^2, respectively. The TiO_2 and ZnO film coated tubings were used as batch reactors for photocatalytic activity measurements. We have also used as a reference, a third tubing without any film, but containing 40 mg of P-25. Finally, a last tubing, with neither film nor P-25, was used as a control to evaluate the effect of photolysis. The mass quantity of P-25 used in the third tubing was of the same order as the mass of the TiO_2 films prepared by SP. The TiO_2 powder was spread out on the bottom surface of the internal wall of the tubing; only a small portion of the bottom surface was covered.

The reaction gas mixture was made with ambient air and 3 ml of diluted butane (Praxair, 10 vol.% butane in helium). The tubing was sealed with a high-vacuum nipple and a septum port; subsequently, after nonleakage was checked, the reaction gas was injected. The tubes were stored for 16–24 h in a dark chamber, before exposition to sunlight. After that, the initial concentration of each reactor gas was verified in order to have 3.03 mol dm^{-3}. To monitor the exposure of the reactors to sunlight in a horizontal plane, 0.1 cm3 of gas sample were taken with a gastight syringe every 15 min. The butane conversion rate was determined in each case using a Perkin Elmer, Autosystem XL gas chromatograph equipped with a thermal conductivity detector. The separation column was a Porapack Q (2 m lengthx3.2 mm o.d.).

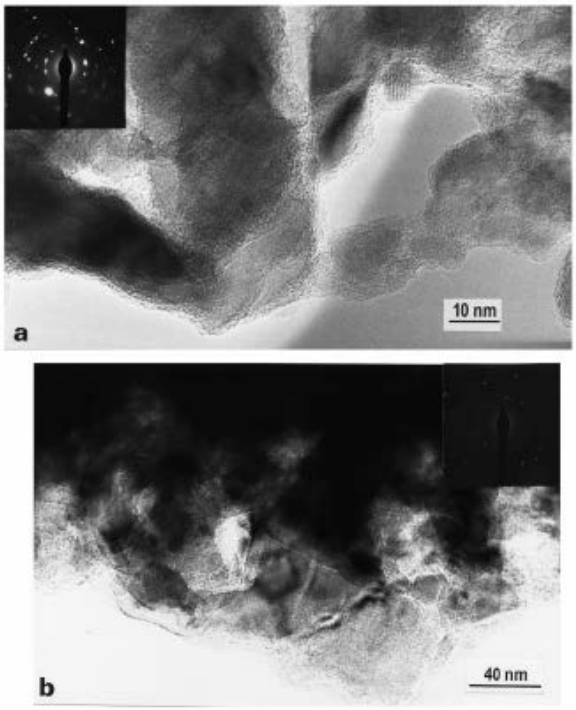

Fig. 2. Bright field TEM micrographs of titanium oxide (a) and zinc oxide (b) films peeled off from the Vycor tubing. Inset shows SAED pattern of the films.

The solar radiation intensity was measured by means of a radiometer model UVP-UVX. Due to the fact that intensity was not constant during each activity test the radiant flux was measured periodically in order to evaluate the average radiant flux.

Results

Thin film characterization: Fig. 2 shows TEM micrographs of titanium oxide (a) and zinc oxide films (b); the SAED patterns of each film are shown in the inset. It can be concluded that titanium oxide films are polycrystalline and their structure corresponds to the tetragonal anatase phase [19]. In addition, ZnO films are also polycrystalline with a structure that belongs to the hexagonal Wurtzite type w20x. Table 1 shows the interplanar distance calculated from these patterns. The agreement between calculated values and those reported in the references is evident.

Table 1
Comparison of interplanar distances obtained from SAED patterns of TiO_2 and ZnO films (Fig. 2) and those reported by the Joint Committee on Powder Diffraction Standards, cards 21-1272 and 36-1451, respectively

TiO_2			ZnO		
(h k l)	d_{ICDD}[a] (nm)	d_{exp} (nm)	(h k l)	d_{ICDD}[b] (nm)	d_{exp} (nm)
(1 0 1)	0.3520	0.359	(1 0 0)	0.2814	0.284
(1 0 3)	0.2431	0.241	(0 0 2)	0.2603	0.263
(0 0 4)	0.2378	0.238	(1 0 1)	0.2476	0.249
(2 0 0)	0.1892	0.193	(1 0 2)	0.1911	0.192
(1 0 5)	0.1700	0.173	(1 1 0)	0.1625	0.163
(1 1 6)	0.1364	0.139	(1 0 3)	0.1477	0.148
(1 0 7)	0.1280	0.128	(1 1 2)	0.1378	0.138

[a] Ref. [19].
[b] Ref. [20].

Fig. 3 shows the transmittance spectra, for external incidence of bare Vycor tubing and for those covered with TiO_2 and ZnO films. From these spectra, film thickness and refraction index were determined by the well-known interference fringes method [21]. We have obtained a thickness of 350 nm for TiO_2 and 330 nm for ZnO films. For ZnO films, absorption edge shifts towards longer wavelength and the transmittance approaches near 0 at approximately 370 nm. Transmittance in visible spectrum of the bare Vycor tubing is approximately 82%, almost 10% lower than that reported for vitreous silica glass [22]. This reduction can be attributed to scattering and refraction due to the curvature of the tubing.

Photocatalytic activity: Fig. 4 shows typical experimental data, of butane conversion as a function of irradiance time. Measurements of the control tubing are not included because no photolysis was detected for butane degradation.

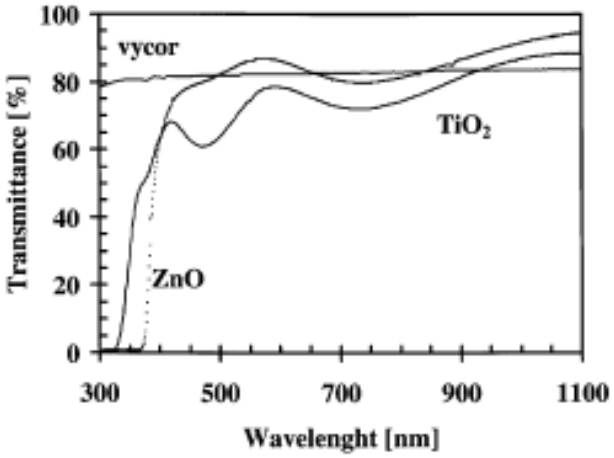

Fig. 3. Transmittance spectra of the uncovered, TiO_2- and ZnO-covered tubing.

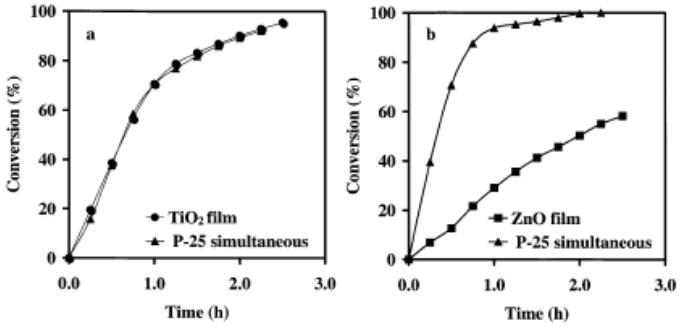

Fig. 4. Butane conversion as a function of irradiance time. (a) For TiO_2-coated tubing (●), compared with P-25 powder (▲), at an average irradiance of 1.10 mW cm^{-2}; and (b) for ZnO film coated tubing (■), compared with P-25 powder (▲), at an average irradiance of 1.23 mW cm^{-2}.

It can be observed in Fig. 4a that TiO_2-coated tubing presented almost the same activity as P-25, i.e. approximately 90% of conversion at 2 h. This outcome was also reported for TiO_2 thin films prepared by sputtering when they were compared with TiO_2 powders [23]. The results of ZnO film and P-25 simultaneous tests are presented in Fig. 4b; the photocatalytic activity of ZnO film is observed to be lower than that of P-25, which presented 50 and 99% of conversion at 2 h, respectively. Differences in P-25 activity (Fig. 4a and b) are partially explained because of the lower mean UVradiant flux

for the activity evaluation made with TiO_2 film (1.0 ± 0.1 mW cm^{-2}) than that with ZnO film (1.5±0.3 mW cm^{-2}) [5,24] and to variations in environmental conditions, principally relative humidity. The reaction rate order was obtained from the extent of reaction according to the butane concentration evolution during the exposition of reactor to solar radiation. The data were fit according to a general power model:

$$r=kC^n$$

where r is the reaction rate, k is the reaction rate constant, C is the butane concentration, and n is the reaction order. The best fitting was obtained for a pseudo-first order rate constant as reported for aqueous phenol degradation over TiO_2 films [23]. Semi-logarithmic plots of concentration ratio (C_0y/C: where C_0 is the initial concentration of butane) as a function of irradiation time are shown in Fig. 5. Fig. 5a corresponds to TiO_2 film and Fig. 5b to ZnO film with their respective P-25 reference. The values obtained for pseudo-first order rate constants (k), pseudo-first order rate constants per unit of surface area (k_s), and pseudo-first order rate constants per unit of mass (k_m) are listed in Table 2. It can be seen that the k value for TiO_2 film (1.23 h^{-1}) was higher than that of P-25 (1.16 h^{-1}) for the same illumination.

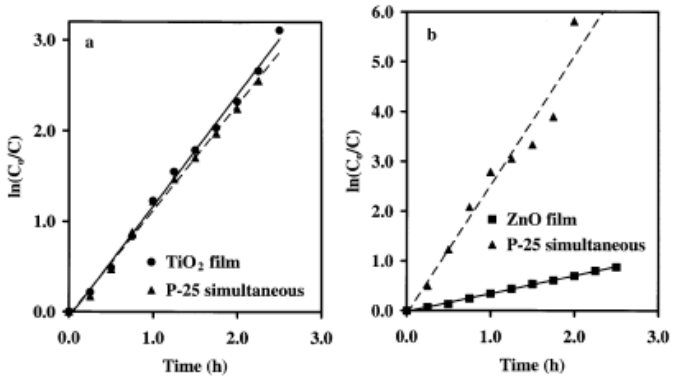

Fig. 5. Semi-logarithmic plots of concentration ratio C_0/C, where C_0 is the initial concentration of butane, as a function of irradiation time; obtained from conversion changes data. (a) For TiO_2 film (●) compared with P-25 powder (▲); and (b) for ZnO film (■) compared with P-25 powder (▲).

Table 2
Pseudo-first order rate constants (k), pseudo-first order rate constants (k_s) per unit of surface area, and pseudo-first order rate constants (k_m) per unit of mass obtained from the least square fittings of the semi-logarithmic plots of concentration ratio (C_0/C) as a function of irradiation time

Material	k (h^{-1})	k_s ($h^{-1}\ m^{-2}$)	k_m ($h^{-1}\ g^{-1}$)
TiO_2 film	1.23	65.8	43.9
P-25 sim. w/TiO_2	1.16	0.6	29.0
ZnO film	0.36	19.3	10.3
P-25 sim. w/ZnO	2.57	1.3	64.3

The k value obtained for ZnO film (0.36 h^{-1}) was three times lower than that of TiO_2, so photocatalytic activity ratio remains as reported before for comparative ZnO and TiO_2 powder studies [24,25]. When k_s is calculated to consider the effect of surface area, thin film materials (65.8 and 19.3 $h^{-1}\ m^{-2}$, for TiO_2 and ZnO, respectively) show more photocatalytic activity than P-25 (0.6 and 1.3 $h^{-1}\ m^{-2}$, for simultaneous measurement with TiO_2 and ZnO, respectively). The surface area, for P-25, was taken as 50 $m^2\ g^{-1}$, which certainly was the total surface of TiO_2 powder per gram, but not the entire surface that played a role in the absorption of UVradiation. For this reason, it is convenient to include the rate constants per unit of mass (k_m), as a better parameter to compare the performance of thin films vs. powder catalysts. Consequently, considering the catalyst gram per gram, TiO_2 is more active in film (43.9 $h^{-1}\ g^{-1}$) than in powder form (29.0 $h^{-1}\ g^{-1}$) under the same UV radiant flux, in spite of this, the film had a much lower surface area. This fact can be deduced if we compare the k_m values (Table 2). However, it should be pointed out that evaluation of rate constants can serve as guidance for the comparison of the relative efficiency of the different systems only under

the particular experimental conditions used (geometric configuration, illumination intensity, reactor gas concentration, catalyst quantity, film thickness, etc.).

Conclusions

The feasibility of depositing transparent, and nonlight scattering thin films of TiO_2 and ZnO inside Vycor tubing has been demonstrated by a simple and reproducible SP technique. TiO_2- convered tubing shows very high photocatalytic activity (k_m=43.9 h^{-1} g^{-1}), higher than that of P-25 (k_m =29.0 h^{-1} g^{-1}), if the activity per m unit of catalyst mass is considered. These results support the viability of the SP technique and expand the possibility of its use in the development of cylindrical reactors for photocatalytic applications.

Acknowledgments

The authors would like to thank R. Ortega, F. Reyes, F. Paraguay, W. Antu´nez, P. Castillo, D. Lardizabal, S. Miranda, and R. Guerrero for their technical assistance. This work was partially supported by a grant from CONACYT project No. 34325-U.

References

1.- A. Fujishima, K. Honda, Nature 238 (1972) 37.

2.- M.Z. Atashbar, H.T. Sun, B. Gong, W. Wlodarski, R. Lamb. Thin Solid Films 326 (1998) 238.

3.- K. Zakrzewska, M. Radecka, M. Rekas, Thin Solid Films 310 (1997) 161.

4. - Y. Paz, A. Heller, J. Mater. Res. 12 (1997) 2759, References therein.

5.- J.-M. Herrmann, Catal. Today 53 (1) (1999) 115.

6.- K. Sunada, Y. Kikuchi, K. Hashimoto, A. Fujishima, Environ. Sci. Technol. 32 (5) (1998) 726.

7.- W.A. Jacoby, P. Ching Maness, E.J. Wolfrum, D.M. Blake, J.A. Fennell, Environ. Sci. Technol. 32 (17) (1998) 2650.

8.- A. Fujishima, T.N. Rao, D.A. Tryk, J. Photochem. Photobiol. C 1 (2000) 1

9.- J.A. Navío, G. Colo´n, M. Mac´ıas, C. Real, M.I. Litter, Appl. Catal. A 177 (1999) 111.

10.- V. Gauthier, S. Bourgeois, P. Sibillot, M. Maglione, M. Sacilotti, Thin Solid Films 340 (1999) 175.

11.- H. Takikawa, T. Matsui, T. Sakakibara, A. Bendavid, P.J. Martin, Thin Solid Films 348 (1999) 145.

12.- Y. Leprince-Wang, K. Yu-Zhang, V. Nguyen Van, D. Souche, J. Rivory, Thin Solid Films 307 (1997) 38.

13.- M. Strømme, A. Gutarra, G.A. Niklasson, C.G. Granqvist, J. Appl. Phys. 79 (7) (1996) 3749.

14.- H. Lindstro¨m, A. Holmberg, E. Magnusson, S.-E. Lindquist, L. Malmqvist, A. Hagfeldt, Nanoletters 1 (2001) 97.

15.- C. Natarajan, N. Fukunaga, G. Nogami, Thin Solid Films 322 (1998) 6.

16.- W.A. Badawy, J. Mater. Sci. 32 (1997) 4979.

17.- P.S. Patil, Mater. Chem. Phys. 59 (1999) 185.

18.- K. Tanaka, K. Abe, T. Hisanga, J. Photochem. Photobiol. A 101 (1996) 85.

19.- Powder Diffraction File, Joint Committee on Powder Diffraction Standards, ICDD, Swarthmore, PA, 1996, Card 21-1272.

20.- Powder Diffraction File, Joint Committee on Powder Diffraction Standards, ICDD, Swarthmore, PA, 1996, Card 36-1451.

21.- O.S. Heavens, Optical Properties of Thin Solid Films, Dover Publications, New York, 1991, p. 115.

22.- M.M. Rahman, K.M. Krishna, T. Soga, T. Jimbo, M. Umeno, J. Phys. Chem. Solids 60 (1999) 201.

23.- D. Dumitriu, A.R. Bally, C. Ballif, P. Hones, P.E. Schmid, R. Sanjine´s, F. Le´vy, V.I. Paˆrvulescu, Appl. Catal. B 25 (2000) 83.

24.- C. Kormann, D.W. Bahnemann, M.R. Hoffmann, J. Photochem. Photobiol. A 48 (1989) 161.

25.- R. Borello, C. Minero, E. Pramauro, E. Pelizzeti, N. Serpone, H. Hidaka, Environ. Toxicol. Chem. 8 (1989) 997.